

Application of Hyperbolic Two-fluids Equations to Reactor Safety Code

Hogon Lim and Unchul Lee

Seoul National University
San56-1 shilnim, Kwanak, Seoul, Korea
ex-hglim@kaeri.re.kr

Kyungdoo Kim and Won-Jae Lee

Korea Atomic Energy Research Institute
150 Dukjin-dong, Yuseung-gu, Daejeon 305-353, Korea

(Received September 10, 2002)

Abstract

A hyperbolic two-phase, two-fluid equation system developed in the previous work has been implemented in an existing nuclear safety analysis code, MARS. Although the implicit treatment of interfacial pressure force term introduced in momentum equation of the hyperbolic equation system is required to enhance the numerical stability, it is very difficult to implement in the code because it is not possible to maintain the existing numerical solution structure. As an alternative, two-step approach with stabilizer momentum equations has been selected. The results of a linear stability analysis by Von-Neumann method show the equivalent stability improvement with fully-implicit solution method. To illustrate the applicability, the new solution scheme has been implemented into the best-estimate thermal-hydraulic analysis code, MARS. This paper also includes the comparisons of the simulation results for the perturbation propagation and water faucet problems using both two-step method and the original solution scheme.

Key Words : hyperbolic, two-fluid equation, interfacial pressure force, MARS, stability, two-step method

I. Introduction

For thermal-hydraulic modeling of two-phase flow systems, separated flow model so called two-fluid model are widely used in nuclear reactor safety analysis codes[8, 10]. Single pressure assumption that the pressures of liquid, vapor, and interface are identical is commonly adopted for

equation system closure. It is well known that typical two-phase flow models with a single pressure assumption possess complex characteristics that may result in system being ill-posed [1]. Consequently, typical six-equation models may cause the unbounded growth of instabilities. In order to mitigate these instabilities, a hyperbolic equation system was proposed by

introducing new interfacial pressure force terms into the single-pressure two-fluid equations [2]. Stuhmiller[3] has searched similar interfacial pressure force terms under the incompressible flow condition and these terms are being used in the CATHARE code. However, these terms do not render single pressure model hyperbolic in the real flow conditions. In this work, new equation system is implemented to a reactor safety analysis code, MARS [5]. Two-step method was chosen as numerical scheme and stability analysis was carried out for two-step method to confirm the degree of stability enhancement compared to implicit numerical method. Although the implicit treatment of interfacial pressure force terms introduced in momentum equations may be required to enhance the numerical stability, two-step solution scheme with stabilizer momentum equations has been selected as an alternative, which maintains the existing numerical solution structure. The result of locally linearized stability analysis by Von-Neumann method [4] shows that the equivalent stability improvement is ensured with that of implicit solution method. Then, two benchmarking problems of wave perturbation and water faucet are performed to evaluate the numerical stability and accuracy of present model.

2. Two Step Method

The previously developed phasic momentum equations for two-fluid model is as follows

$$\alpha_k \rho_k \frac{\partial v_k}{\partial t} + \frac{1}{2} \alpha_k \rho_k \frac{\partial v_k^2}{\partial x} + \alpha_k \frac{\partial p}{\partial x} + \Delta p \frac{\partial \alpha_k}{\partial x} = M_{ik}, \quad k = f, g \quad (1)$$

where

$$\Delta p = \left(1 + \frac{(\alpha_f c_g^2 + \alpha_g c_f^2)(v_g - v_f)^2}{c_f^2 c_g^2 - (\alpha_f c_g^2 + \alpha_g c_f^2)(v_g - v_f)^2} \right) \left(\frac{\alpha_f \alpha_g \rho_g \rho_f}{\alpha_f \rho_g + \alpha_g \rho_f} \right) (v_g - v_f)^2.$$

M_{ik} indicates non-differential terms such as wall and interfacial drag, vapor generation and body force. Fourth term of left-hand side indicates

interfacial pressure force. For the easy decoupling of momentum equation with mass and energy equations, the MARS code limits the implicitness of difference momentum equation. New time-step values of phasic velocity in the resulting difference momentum equation should be expressed as a function of pressures only. However, explicit treatment of interfacial pressure force term cannot guarantee overall stability enhancement. As an alternative, two-step method was chosen to maintain existing solution procedure of MARS and enhance the stability by increasing the implicitness of interfacial pressure force difference term. In the basic step, interfacial pressure force term is differenced explicitly and subsequent difference momentum equations are expressed as a function of pressure as in the original equations of MARS. Resulting difference equations of momentum, mass, and energy are as follows:

Basic step:

phasic momentum:

$$\begin{aligned} & \left(\overline{\alpha_k \rho_k} \right)_{j+1/2}^n \frac{\tilde{v}_{k,j+1/2}^{n+1} - v_{k,j+1/2}^n}{\Delta t} + \frac{1}{2} \left(\overline{\alpha_k \rho_k} \right)_{j+1/2}^n \frac{(v_{k,j+1}^n)^2 - (v_{k,j}^n)^2}{\Delta x} \\ & + \alpha_{k,j+1/2}^{n+1} \frac{p_{j+1}^{n+1} - p_j^{n+1}}{\Delta x} + (\Delta p)_{j+1/2}^n \frac{\alpha_{k,j+1}^{n+1} - \alpha_{k,j}^{n+1}}{\Delta x} = M_{ik}^{n+1} \end{aligned} \quad (2)$$

phasic mass:

$$\begin{aligned} & \frac{\rho_k}{\Delta t} (\alpha_{k,j}^{n+1} - \alpha_{k,j}^n) + \frac{\alpha_{k,j}^n}{\Delta t} (\rho_{k,j}^{n+1} - \rho_{k,j}^n) \\ & + \frac{((\dot{\alpha}_k \dot{\rho}_k)_{j+1/2}^n \tilde{v}_{k,j+1/2}^{n+1} - (\dot{\alpha}_k \dot{\rho}_k)_{j-1/2}^n \tilde{v}_{k,j-1/2}^{n+1})}{\Delta x} = \Gamma_{k,j}^n \end{aligned} \quad (3)$$

phasic energy:

$$\begin{aligned} & ((\rho_k U_k)_{j+1/2}^n + p_j^n) \frac{\alpha_{k,j}^{n+1} - \alpha_{k,j}^n}{\Delta t} + (\alpha_k U_k)_{j+1/2}^n \frac{\rho_{k,j}^{n+1} - \rho_{k,j}^n}{\Delta t} + (\alpha_k \rho_k)_{j+1/2}^n \frac{U_{k,j}^{n+1} - U_{k,j}^n}{\Delta t} \\ & + \frac{(\dot{\alpha}_k \dot{\rho}_k \dot{U}_k)_{j+1/2}^n \tilde{v}_{k,j+1/2}^{n+1} - (\dot{\alpha}_k \dot{\rho}_k \dot{U}_k)_{j-1/2}^n \tilde{v}_{k,j-1/2}^{n+1}}{\Delta x} \\ & + p_j^n \frac{\dot{\alpha}_{k,j+1/2}^{n+1} \tilde{v}_{k,j+1/2}^{n+1} - \dot{\alpha}_{k,j-1/2}^{n+1} \tilde{v}_{k,j-1/2}^{n+1}}{\Delta x} = Q_{ik}^{n+1} + Q_{ik}^{n+1} + \Gamma_{ik}^n h_k^n \end{aligned} \quad (4)$$

The values having bar on top in the difference momentum equation (2) denote average value of neighboring scalar cells and the values having a dot on top are donored quantities based on phasic

velocities, $\tilde{v}_{g,j}$ and $\tilde{v}_{l,j}$. Values having tilde on top means tentative variables. Solution procedure used in the MARS code is adopted for solving dependent variables, p , α_k , U_k , and \tilde{v}_j . Tentative phasic velocities are subsequently updated in stabilizing step based on the new time-step values of void fractions. Resulting stabilizer momentum equations at stabilizing step are written as follows:

$$\begin{aligned} & \left(\overline{\alpha_k \rho_k}\right)_{j+1/2}^n \frac{v_{k,j+1/2}^{n+1} - v_{k,j+1/2}^n}{\Delta t} + \frac{1}{2} \left(\overline{\alpha_k \rho_k}\right)_{j+1/2}^n \frac{(v_{k,j+1}^n)^2 - (v_{k,j}^n)^2}{\Delta x} \\ & + (\Delta p)_{j+1/2}^n \frac{\alpha_{k,j+1}^{n+1} - \alpha_{k,j}^{n+1}}{\Delta x} = -\alpha_{k,j+1/2}^{n+1} \frac{p_{j+1}^{n+1} - p_j^{n+1}}{\Delta x} + M_{ik}^{n+1} \end{aligned} \quad (5)$$

Because all variables except velocities are already calculated in the basic step, equation (5) is simple algebraic equation. Therefore, adding stabilizing step does not influence the calculational efficiency of code.

3. Numerical Stability Analysis

To investigate the numerical stability of the two-step method, Von-Neumann stability analysis was performed [4, 9]. For simplification, the following conditions were used.

- (1) Exclusion of lower order terms as well as source terms
- (2) Exclusion of energy equations

Lower order terms such as wall friction and interfacial drag are generally considered to have positive influence on stability [6]. Also, energy equation imposes the condition so called Courant limit. Courant limit is used as limit condition of present stability analysis. The resultant phasic mass and momentum equations can be written as:

Basic mass equation:

$$\begin{aligned} & \rho_k \left[\frac{\alpha_{k,j}^{n+1} - \alpha_{k,j}^n}{\Delta t} \right] + \frac{\alpha_{k,j}^n}{c_k^2} \left[\frac{p_{j+1}^{n+1} - p_j^{n+1}}{\Delta t} \right] + (\rho_k v_k)^n \left[\frac{\alpha_{k,j}^{n+1} - \alpha_{k,j}^n}{\Delta x} \right] \\ & + \left(\frac{\alpha_k v_k}{c_k^2} \right) \left[\frac{p^{n+1} - p^n}{\Delta x} \right] + (\rho_k \alpha_k)^n \left[\frac{\tilde{v}_{k,j+1/2}^{n+1} - \tilde{v}_{k,j-1/2}^{n+1}}{\Delta x} \right] = 0 \end{aligned} \quad (6)$$

Basic phasic momentum equation:

$$\begin{aligned} & (\alpha_k \rho_k)^n \left[\frac{\tilde{v}_{k,j+1/2}^{n+1} - v_{k,j-1/2}^n}{\Delta t} \right] + (\alpha_k \rho_k v_k)^n \left[\frac{v_{k,j}^n - v_{k,j-1}^n}{\Delta x} \right] \\ & (\alpha_k)^n \left[\frac{p_{j+1}^{n+1} - p_j^{n+1}}{\Delta x} \right] + (\Delta p)^n \left[\frac{\alpha_{k,j+1}^n - \alpha_{k,j}^n}{\Delta x} \right] = 0 \end{aligned} \quad (7)$$

Stabilizing momentum equation:

$$\begin{aligned} & (\alpha_k \rho_k)^n \left[\frac{v_{k,j+1/2}^{n+1} - v_{k,j-1/2}^n}{\Delta t} \right] + (\alpha_k \rho_k v_k)^n \left[\frac{v_{k,j}^n - v_{k,j-1}^n}{\Delta x} \right] \\ & (\alpha_k)^n \left[\frac{p_{j+1}^{n+1} - p_j^{n+1}}{\Delta x} \right] + (\Delta p)^n \left[\frac{\alpha_{k,j+1}^{n+1} - \alpha_{k,j}^{n+1}}{\Delta x} \right] = 0 \end{aligned} \quad (8)$$

where the subscript k denotes 'g' and 'f' for vapor and liquid phases, respectively.

To investigate the stability of numerical scheme, dependent variables are expressed as wave component that has frequency of 'k', that is

$$\Phi_j' = \hat{\Phi}'(k) e^{ikx} \quad (9)$$

Using equation(9), equations(6)-(8) are rewritten as:

Basic step mass equation:

$$\begin{aligned} & \rho_k \alpha_k^{i+\Delta t} + \frac{\alpha_k}{c_k^2} p^{i+\Delta t} + \alpha_k \rho_k \frac{\Delta t}{\Delta x} ik \tilde{v}_k^{i+\Delta t} \\ & = \rho_k (1 - \bar{v}_k) \delta \alpha_k' + \frac{\alpha_k}{c_k^2} (1 - \bar{v}_k) \delta p' \end{aligned} \quad (10)$$

Basic step momentum equation

$$\begin{aligned} & \alpha_k \rho_k \tilde{v}_k^{i+\Delta t} + \alpha_k \frac{\Delta t}{\Delta x} ik p^{i+\Delta t} \\ & = \alpha_k \rho_k (1 - \bar{v}_k) v_k' - \Delta p \frac{\Delta t}{\Delta x} ik \alpha_g' \end{aligned} \quad (11)$$

Stabilizing momentum equation

$$\begin{aligned} & \Delta p \frac{\Delta t}{\Delta x} ik \alpha_k^{i+\Delta t} + \alpha_k \rho_k v_k^{i+\Delta t} + \alpha_k \frac{\Delta t}{\Delta x} ik p^{i+\Delta t} \\ & = \alpha_k \rho_k (1 - \bar{v}_k) \delta v_k' \end{aligned} \quad (12)$$

where $\bar{v}_k = v_k \frac{\Delta t}{\Delta x} (1 - e^{-ik\Delta x})$, $k' = 2 \sin(k\Delta x/2)$

In case that U is a vector containing six

amplitudes of the dependent variables, $\alpha_g, p, \tilde{u}_g, \tilde{v}_f, v_g$ and v_f , equation (10) through (12) for each phase can be written in the form of.

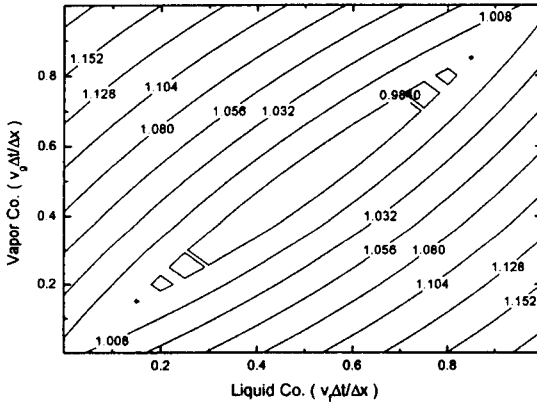
$$A U^{(n+1)} = B U^{(n)}$$

$$A = \begin{pmatrix} \rho_g & \frac{\alpha_g}{c_g^2} & \alpha_g \rho_x \frac{\Delta t}{\Delta x} ik' & 0 & 0 & 0 \\ -\rho_f & \frac{\alpha_f}{c_f^2} & 0 & \alpha_f \rho_f \frac{\Delta t}{\Delta x} ik' & 0 & 0 \\ 0 & \alpha_x \frac{\Delta t}{\Delta x} ik' & \alpha_g \rho_g & 0 & 0 & 0 \\ 0 & \alpha_f \frac{\Delta t}{\Delta x} ik' & 0 & \alpha_f \rho_f & 0 & 0 \\ \Delta p \frac{\Delta t}{\Delta x} ik' & \alpha_x \frac{\Delta t}{\Delta x} ik' & 0 & 0 & \alpha_g \rho_g & 0 \\ -\Delta p \frac{\Delta t}{\Delta x} ik' & \alpha_f \frac{\Delta t}{\Delta x} ik' & 0 & 0 & 0 & \alpha_f \rho_f \end{pmatrix}$$

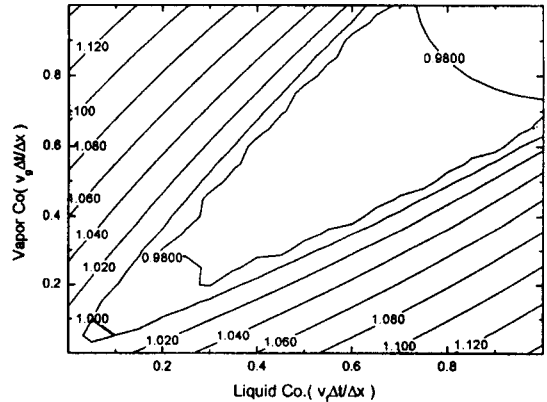
$$B = \begin{pmatrix} \rho_g(1-\tilde{v}_g) \frac{\alpha_g}{c_g^2}(1-\tilde{v}_g) & 0 & 0 & 0 & 0 \\ -\rho_f(1-\tilde{v}_f) \frac{\alpha_f}{c_f^2}(1-\tilde{v}_f) & 0 & 0 & 0 & 0 \\ -\Delta p \frac{\Delta t}{\Delta x} ik' & 0 & 0 & \alpha_g \rho_g(1-\tilde{v}_g) & 0 \\ \Delta p \frac{\Delta t}{\Delta x} ik' & 0 & 0 & 0 & \alpha_f \rho_f(1-\tilde{v}_f) \\ 0 & 0 & 0 & \alpha_g \rho_g(1-\tilde{v}_g) & 0 \\ 0 & 0 & 0 & 0 & \alpha_f \rho_f(1-\tilde{v}_f) \end{pmatrix}$$

$$U = (\alpha_x \quad p \quad \tilde{v}_g \quad \tilde{v}_f \quad v_g \quad v_f)^T$$

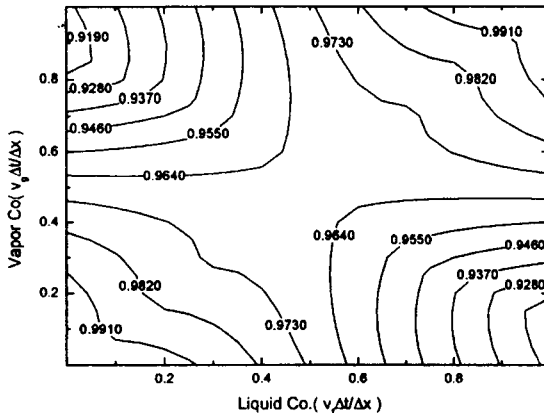
The condition for stability is that the eigenvalues of the amplification matrix $G = A^{-1}B$ must be equal to or less than 1. The eigenvalues are the roots of the characteristic polynomial equation, $|A\lambda - B| = 0$, that is:



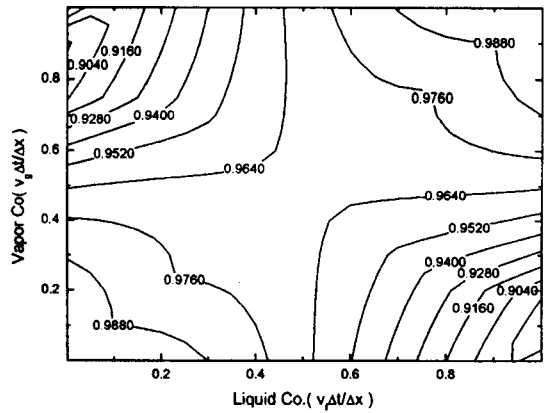
(a) Basic model



(b) MARS default



(c) Implicit differencing



(d) Two-step method

Fig. 1. Spectral Radius Contour for the Compressible Flow Condition
 $\tilde{C}_g = 1, \tilde{c}_l = 5, k\Delta x = \pi/6, \epsilon = 1, \alpha_g = 0.5$

$$\left\{ \Lambda_f^2 \Lambda_f^2 + k'^2 \bar{c}^2 \lambda^2 \left(\left(1 + \kappa_p \frac{\alpha_g}{c_g^2} \right) \Lambda_f^2 + \left(\varepsilon^2 + \kappa_p \frac{\alpha_f}{c_f^2} \right) \Lambda_g^2 \right) \right\} + (13)$$

$$\kappa_p \bar{c}^2 k'^2 (1 - \lambda) \left\{ \Lambda_k \Lambda_f \left(\frac{\alpha_f}{c_f^2} \Lambda_g + \frac{\alpha_g}{c_g^2} \Lambda_f \right) + \lambda^2 (\alpha_f \Lambda_g + \alpha_g \Lambda_f) \right\}$$

$$+ \kappa_p \bar{c}^2 k'^4 \lambda^4 = 0$$

where $\Lambda_k \equiv \lambda - 1 + \tilde{v}_k$, $\varepsilon^2 \equiv \frac{\alpha_f \rho_g}{\alpha_g \rho_f}$, $\hat{c}_k \equiv c_k \frac{\Delta t}{\Delta x}$,
 $\kappa_p \equiv \frac{\Delta p}{\alpha_g \rho_f \Delta x^2}$, and $\bar{c}^2 \equiv \frac{\hat{c}_g^2 \hat{c}_f^2}{\hat{c}_g^2 + \varepsilon^2 \hat{c}_g^2}$

This fourth order characteristic polynomial is too complicated to determine the spectral radius analytically. To examine the effect of the interfacial pressure force, the spectral radius

contour for the two-step method is compared with the implicit treatment of interfacial pressure force in figures 1 and 2 for the representative conditions of compressibility and incompressibility, respectively. Also, the spectral radius contours of the basic and MARS default models are represented to compare the stability with the new model. For small and large phasic sonic speeds, which imply compressible and incompressible conditions, respectively, the spectral radius contours of different numerical treatment of interfacial pressure force are very similar and satisfy the convective limit. Consequently, two-step approach of the interfacial pressure force

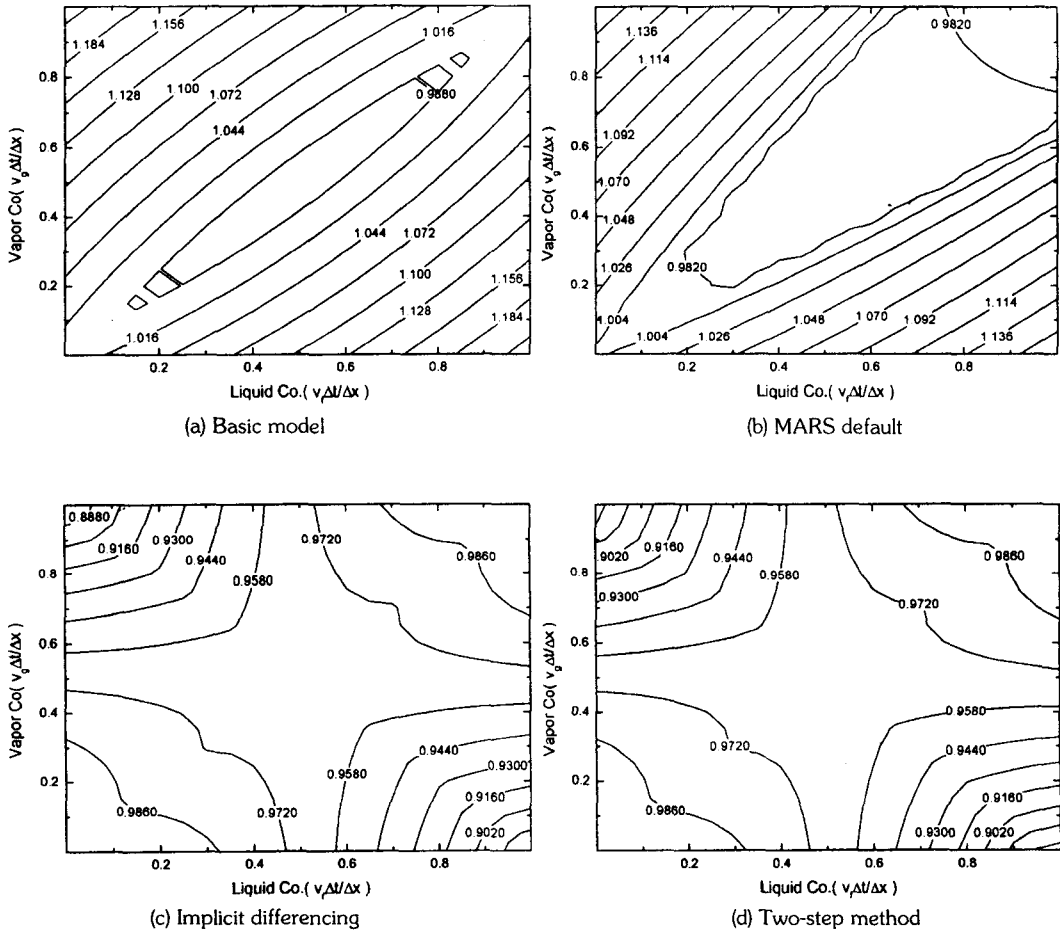


Fig. 2. Spectral Radius Contour for the Incompressible Flow Condition
 $\hat{c}_g = 10^3$, $\hat{c}_l = 5 \times 10^3$, $k\Delta x = \pi/6$, $\varepsilon = 1$, $\alpha_g = 0.5$

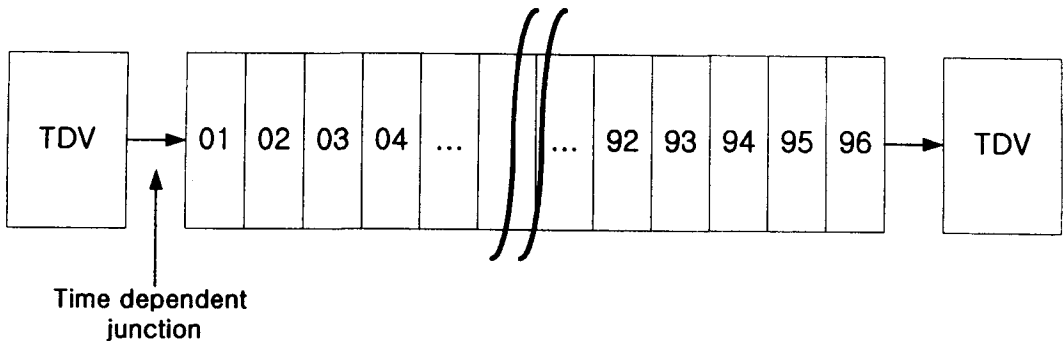


Fig. 3. Nodalization of Horizontal Pipe

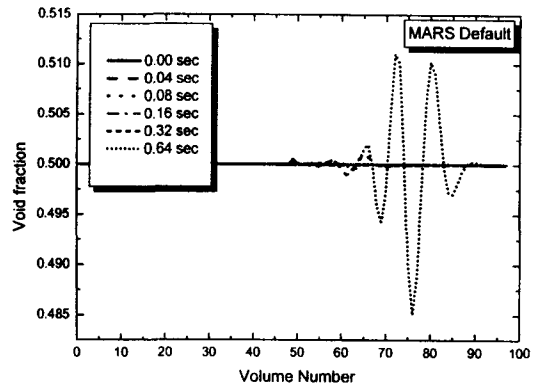
significantly enhances the numerical stability as in the case of implicit treatment.

4. Stability Test Problems

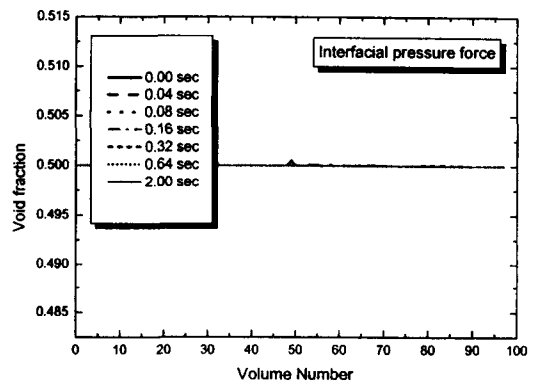
The new hyperbolic model was implemented in a MARS code using two-step method. To examine the stability and accuracy of the present model, a wave perturbation and water faucet problems have been simulated and the results were compared with those of MARS default model. For simplicity, non-differential terms such as wall friction, interfacial drag, and vapor generation have been ignored. As mentioned above chapter, these terms have positive effects in the sense of numerical stability. Details of problem geometry and initial conditions are as follows.

4.1. Wave Perturbation Problem

It is well known that if the system of equations is hyperbolic and a consistent numerical scheme is adapted, a perturbation must be damped along with its propagation due to numerical diffusion. The simulations were carried out for two kinds of waves, having different wavelengths. A horizontal pipe with length of 11m is selected as test geometry and discretized into 96 volumes. The nodalization is shown in Fig. 3. Pipe is initially

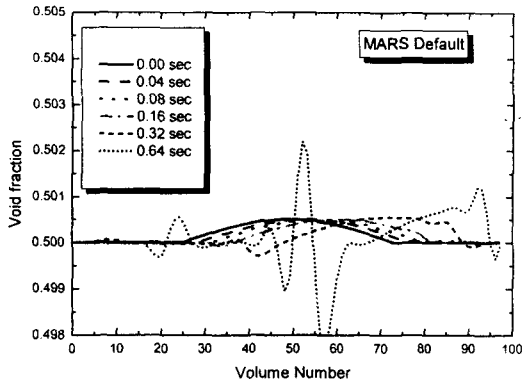


(a) MARS default

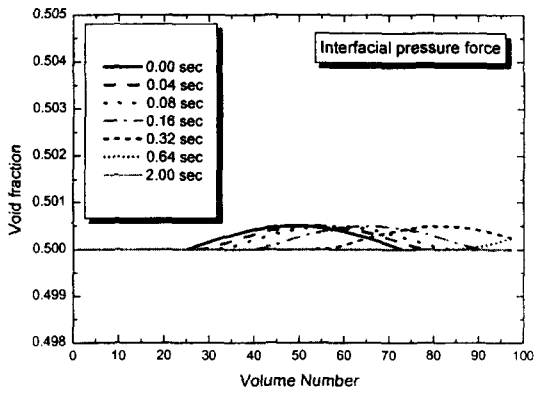


(b) Two-step method

Fig. 4. Short Wavelength Void Perturbation (perturbation wavelength: $1 \times \Delta x$) $v_f = 10\text{m/sec}$, $v_g = 1.0\text{m/sec}$



(a) MARS default model



(b) Present model

Fig. 5. Long Wavelength Void Perturbation (perturbation wavelength: $11 \times \Delta x$) $v_f = 10\text{m/sec}$, $v_g = 1.0\text{m/sec}$

filled with saturated liquid and vapor with a constant void fraction of 0.5. The initial liquid and vapor velocities are 1 m/s and 0.1m/s, respectively. As shown in Figs. 4 and 5, the void perturbation is damped continuously as wave propagates in the new model. On the contrary, the default model shows unstable propagation characteristics. It is thought that the MARS default model has partially elliptic characteristic. From these results, it is obvious that the new model with the interfacial pressure force term has more stable characteristics.

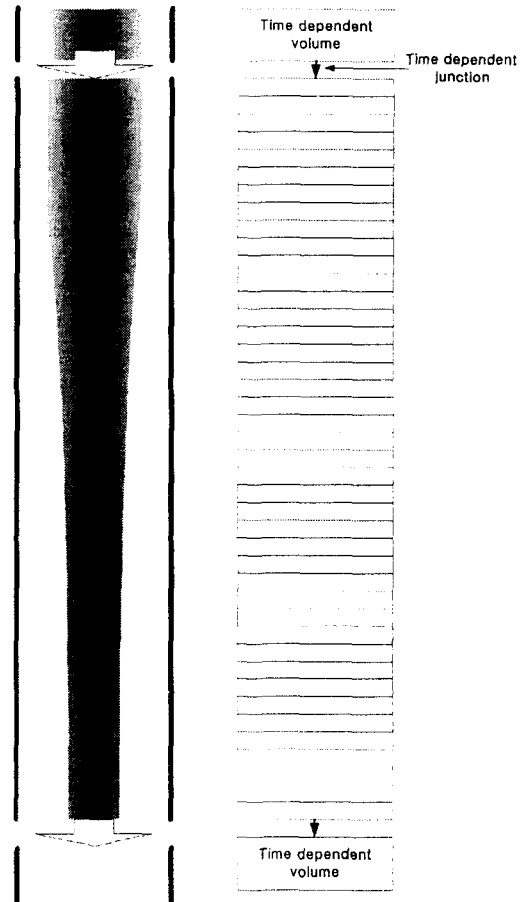


Fig. 6. Schematic and Nodalization of FAUCET Problem

4.2. Water Faucet Problem

In this numerical experiment, the accuracy of the new model is tested. Ransom has developed a two-phase benchmark problem, which has an analytic solution [7]. In his problem, the only driving force is gravity and frictions are ignored. The simulated pipe is a vertical channel with 96 volumes and is about 11m high. The nodalization and schematic diagram are shown in Fig. 6. At the start of the simulation, water falls into the pipe with an initial velocity of 10m/s at the top

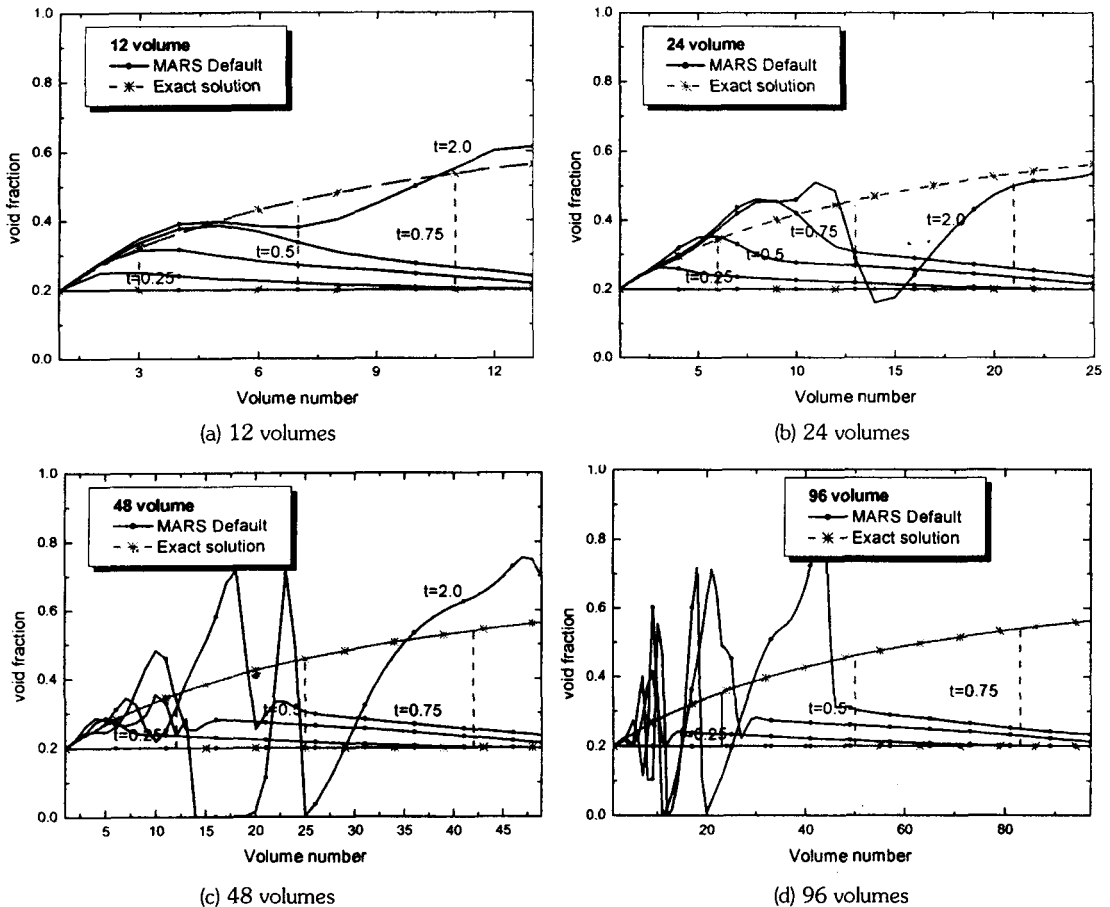


Fig. 7. The Water Faucet Problem(MARS original)

entrance. Then, the falling speed of water is accelerated by gravity. As shown in Figs. 7 and 8, the result of the present model agrees well with the exact solution. Broadening of the void fraction profile at the front of falling water is thought to be due to numerical diffusion.

5. Summary and Conclusions

We implemented the hyperbolic two-phase model to the safety analysis code, MARS, using two-step finite difference scheme to maintain the existing code calculation structure. To examine the numerical stability of this method, a linearized

Von-Neumann stability analysis was carried out. It was shown that stability characteristic of implicit treatment of void derivative is also valid for the two-step method. The solution accuracy and applicability of a developed solution scheme have been demonstrated by the simulation results of the benchmark problem. This model is currently adopted in MARS as an option. Since it is required to perform various test simulations for the new model to be used in real plant safety calculation, many numerical tests including integrated system simulations are now being carried out.

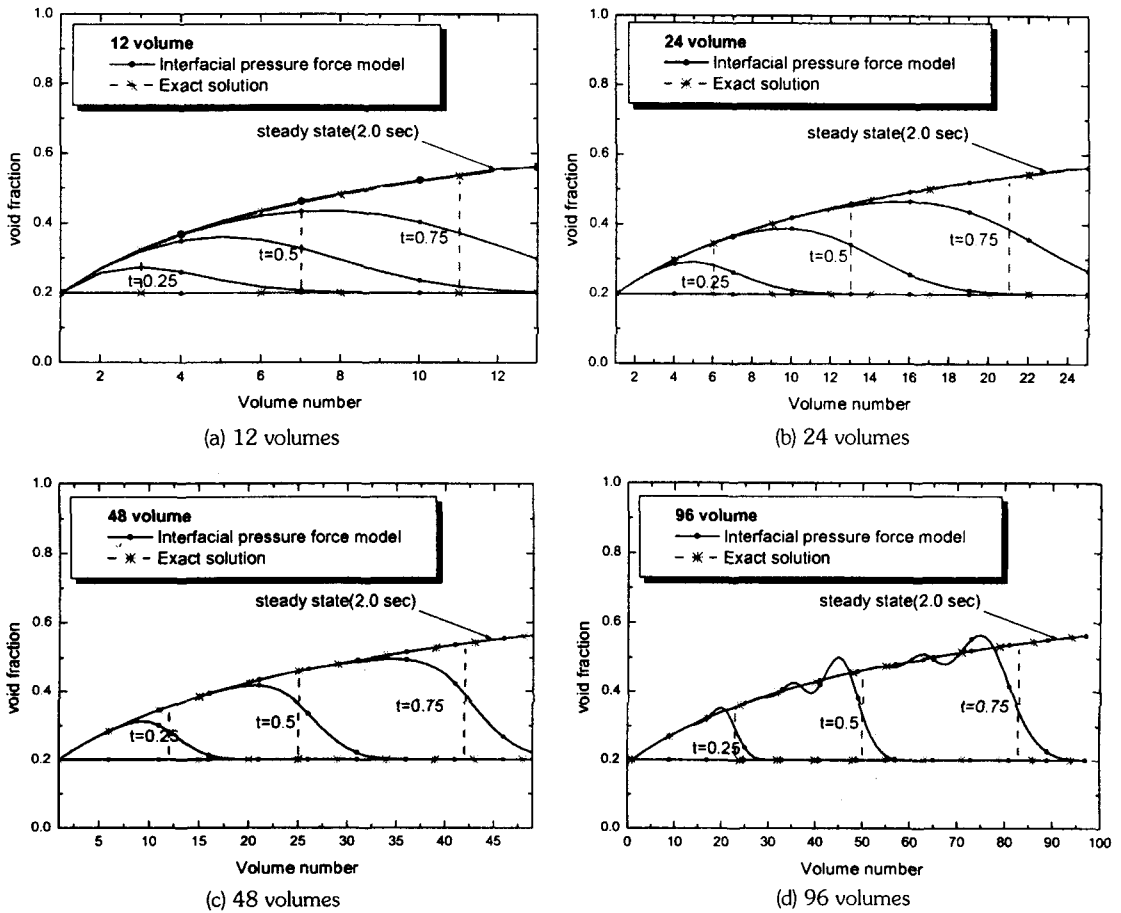


Fig. 8. The Water Faucet Problem (Interfacial pressure force)

Nomenclature

- A flow area
- c sonic speed
- k wave number
- p pressure
- v velocity
- α void fraction
- Δx volume length
- Δt time step size
- Γ vapor generation rate
- ρ mass density
- U internal energy

Subscripts

- f liquid phase
- g vapor phase
- i interface
- m mixture
- j node index

Superscripts

- n time step advancement

Acknowledgments

This work was performed under the Long-term

Nuclear R&D Program sponsored by the Ministry of Science and Technology

References

1. Lyczkowski, R. W., Gidaspow, D., Solbrig, C.W., and Hughes, E. D., 1978, Characteristics and stability analysis of transient one-dimensional two-phase flow equations and their finite difference approximations, *Nucl. Sci. Eng.*, 66, 378.
2. Lim. H. G. et al, 2001, "Application of Stability Enhancing Minimum Interfacial Pressure Force Model for MARS," KAERI/TR-1784/2001.
3. Stuhmiller, J.H., 1977, "The influence of Interfacial Pressure Forces on the Character of the Two-phase Flow model Equations," *Int. J. Multiphase Flow* 3, 551-560.
4. Strikwerda, J. A., 1989, *Finite Difference Schemes and Partial Differential Equations*, Wadsworth & Brooks/Cole Advanced Books & Software Pacific Grove, California.
5. Jeong, J.-J., Ha, K. S., Chung, B. D., Lee, W. J., "Development of A Multi-dimensional Thermal-Hydraulic System Code, MARS 1.3.1," *Annals of Nuclear Energy* 26(18), 1161-1642 (1999).
6. Holmes, M. A., 1995, *Stability of Finite Difference Approximations of Two Fluid, Two Phase Flow Equations*, Ph.D. Thesis, NCSU, Raleigh.
7. Ransom, V. H., 1979, "Faucet Flow, Oscillating Manometer, and Expulsion of Steam by Subcooled Water," Part 3, Numerical Benchmark Tests, *Multiphase Science and Technology*, Volume 3.
8. Carlson, K. E., Riemke, R. A., Rouhani, S.Z., Shumway, R. W., and Weaver, W. L., RELAP5/MOD3 code manual volume 1: code structure, system models, and solution methods (draft), NUREG/CR-5535, EGG-2596, EG&G Idaho, Inc., June (1990).
9. Kim, K. D., Lee, S. J., Chang, W. P., Ha, E. J., Jeun, G. D., 1998, Numerical Stability Analysis of New Hyperbolic Equations for Two-Phase Flow, Proc. 6th International Conference on Nuclear Engineering, San Diego.
10. TRAC-PF1/MOD1: An advanced best-estimate computer program for pressurized water reactor thermal-hydraulic analysis, NUREC/CR-3858, LA-10157-MS, Los Alamos National Laboratory, (1986).